Design of Permanent Magnets to Avoid Chaos in Doubly Salient PM Machines

Y. Gao, *Student Member, IEEE,* and K. T. Chau, *Senior Member, IEEE*

Abstract—This paper analyzes the effect of permanent magnets (PMs) on the formation of chaos in doubly salient PM (DSPM) machines. Based on the newly derived nonlinear system dynamical equation, the corresponding Poincaré map and bifurcation diagram show that the sizing of PMs significantly affects the stability of DSPM machines. Chaos may be resulted if the PMs are not properly designed. Both computer simulations and experimental results are provided to support the theoretical derivation.

Index Terms—Bifurcation, chaos, doubly salient, permanent magnet (PM), Poincaré map.

I. INTRODUCTION

RECENTLY, a new class of brushless machines, termed the doubly salient permanent magnet (DSPM) machine, has been introduced [1]–[3]. The DSPM machine incorporates the merits of both the PM brushless machine and the switched reluctance (SR) machine. Namely, the PMs are located in the stator so that the problems of irreversible demagnetization and mechanical instability can be solved, while the rotor is the same as that of the SR machine so that the advantages of simple configuration and mechanical robustness can be retained. However, this machine still suffers from torque ripples and possible formation of chaos. Those torque ripples can be alleviated by adopting rotor skewing [3], whereas the investigation of its chaotic behavior is not yet explored.

Recent investigations have revealed that chaos occurs in the dc machine [4], induction machine [5], brushless dc machine [6], SR machine [7] and PM synchronous machine [8]. Particularly, the effect of PMs on the formation of chaos in the PM synchronous machine was analyzed in [8]. However, this analysis is ill-suited to the DSPM machine that is directly connected to the power system.

This paper first analyzes the relationship between the sizing of PMs and the formation of chaos in DSPM machines. A practical three-phase 12/8-pole DSPM machine with a skewed rotor structure is used for exemplification. With the use of rotor skewing, the air-gap flux is sinusoidally distributed so that vector control can be employed for high-performance operation. In Section II, a nonlinear system dynamical equation will be derived. Then, Poincaré mapping and bifurcation analysis will be conducted in Section III. Hence, the formation of chaos with respect to the PM flux will be presented in Section IV.
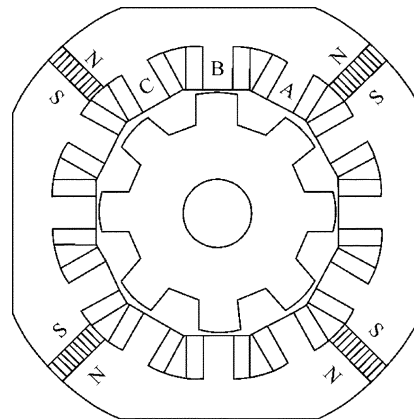
Fig. 1. Three-phase 12/8-pole DSPM machine configuration.

II. SYSTEM DYNAMICS

Fig. 1 shows a three-phase 12/8-pole DSPM machine, which consists of three-phase concentrated windings in the stator, 12 salient poles in the stator, and eight salient poles in the rotor. Its PMs are located in the stator, and there are no windings or PMs in the rotor. With rotor skewing, the PM flux with respect to phases A, B, and C can be approximated as

$$\begin{cases} \psi_{as} = \psi_{\mathrm{pm}} + \psi_a \cos\theta \\ \psi_{bs} = \psi_{\mathrm{pm}} + \psi_a \cos\left(\theta - \frac{2\pi}{3}\right) \\ \psi_{cs} = \psi_{\mathrm{pm}} + \psi_a \cos\left(\theta + \frac{2\pi}{3}\right) \end{cases} \quad (1)$$

where ψ_{pm} is the average PM flux, ψ_a is its amplitude of variations, and θ is the spatial angle with the reference at the aligned position of phase A. Thus, after neglecting magnetic saturation, the self- and mutual inductances of the stator can be written as

$$\begin{cases} L_{aa} = L_{g0} + L_{g2}\cos\theta \\ L_{bb} = L_{g0} + L_{g2}\cos\left(\theta - \frac{2\pi}{3}\right) \\ L_{cc} = L_{g0} + L_{g2}\cos\left(\theta + \frac{2\pi}{3}\right) \end{cases} \quad (2)$$

$$\begin{cases} L_{ab} = L_{ba} = -\frac{L_{g0}}{2} + L_{g2}\cos\left(\theta + \frac{2\pi}{3}\right) \\ L_{bc} = L_{cb} = -\frac{L_{g0}}{2} + L_{g2}\cos\theta \\ L_{ca} = L_{ac} = -\frac{L_{g0}}{2} + L_{g2}\cos\left(\theta - \frac{2\pi}{3}\right) \end{cases} \quad (3)$$

where $L_{g0} = (L_a + L_u)/2$, $L_{g2} = (L_a - L_u)/2$, and L_a and L_u are the inductances at the aligned and unaligned positions, respectively. Hence, the system voltage equation is given by

$$\begin{bmatrix} u_{as} \\ u_{bs} \\ u_{cs} \end{bmatrix} = \begin{bmatrix} -R_s + pL_{aa} & pL_{ab} & pL_{ac} \\ pL_{ba} & -R_s + pL_{bb} & pL_{bc} \\ pL_{ca} & pL_{cb} & -R_s + pL_{cc} \end{bmatrix}$$
$$\cdot \begin{bmatrix} i_{as} \\ i_{bs} \\ i_{cs} \end{bmatrix} - \psi_a n_p \omega_r \begin{bmatrix} \sin\theta \\ \sin\left(\theta - \frac{2\pi}{3}\right) \\ \sin\left(\theta + \frac{2\pi}{3}\right) \end{bmatrix} \quad (4)$$

where p represents the operator d/dt, R_s is the stator resistance, n_p is the number of pole pairs, and ω_r is the rotor speed.

Applying the well-known Park's transformation to (4), the three-phase DSPM machine with rotor skewing can be modeled in $d - q$ frame as given by

$$\begin{cases} L_{ds}\frac{di_{ds}}{dt} = -u_{ds}-R_s i_{ds}+n_p\omega_r L_{qs}i_{qs} \\ L_{qs}\frac{di_{qs}}{dt} = -u_{qs}-R_s i_{qs}-n_p\omega_r L_{ds}i_{ds}+n_p\psi_a\omega_r \\ J\frac{d\omega_r}{dt} = \frac{3}{2}n_p(L_{ds}-L_{qs})i_{ds}i_{qs}-\frac{3}{2}n_p\psi_a i_{qs}-B_m\omega_r+T_m \end{cases} \tag{5}$$

where i_{ds}, i_{qs} are the stator currents, u_{ds}, u_{qs} are the stator voltages, L_{ds}, L_{qs} are the stator inductances, T_m is the mechanical driving torque, J is the rotor inertia, and B_m is the viscosity friction coefficient.

When the DSPM machine is connected to a power system where the frequency is f and the phase voltage amplitude is V, the corresponding u_{ds}, u_{qs} can be expressed as

$$\begin{cases} u_{ds} = V\sin(2\pi ft - \theta + \alpha) \\ u_{qs} = V\cos(2\pi ft - \theta + \alpha) \end{cases} \tag{6}$$

where α is the initial phase angle difference. Substituting (6) into (5), the system dynamical equation can be written as

$$\begin{cases} L_{ds}\frac{di_{ds}}{dt} = -V\sin(2\pi ft-\theta+\alpha)-R_s i_{ds}+n_p\omega_r L_{qs}i_{qs} \\ L_{qs}\frac{di_{qs}}{dt} = -V\cos(2\pi ft-\theta+\alpha)-R_s i_{qs}-n_p\omega_r L_{ds}i_{ds} \\ \qquad\qquad +n_p\psi_a\omega_r \\ J\frac{d\omega_r}{dt} = \frac{3}{2}n_p(L_{ds}-L_{qs})i_{ds}i_{qs}-\frac{3}{2}n_p\psi_a i_{qs}-B_m\omega_r+T_m \\ \frac{d\theta}{dt} = n_p\omega_r. \end{cases} \tag{7}$$

III. POINCARÉ MAP AND BIFURCATION

Poincaré mapping is an effective method that functions to replace the solution of a continuous-time dynamical system by an iterative map. It acts like a stroboscope which produces a sequence of samples of the continuous-time solution. Thus, the steady-state behavior of the Poincaré map, termed the orbit, corresponds to the steady-state waveform of the continuous-time dynamical system.

For a nonautonomous system as described by (7), a natural way to construct the Poincaré map is to sample the trajectory with the power system frequency f. Hence, the Poincaré surface $\sum \in \Re^4 \times S^1$ is defined as

$$\sum := \left\{ (\mathbf{x}, t) \in \Re^4 \times S^1 : t = t_0 \right\} \tag{8}$$

where $\mathbf{x} = [i_{ds}, i_{qs}, \omega_r, \theta]$ is the solution of the state vector. The trajectory of $\mathbf{x}(t)$ repeatedly passes the surface $\sum$ for every period T (namely, the period of the power system). The sequence of surface crossings, so-called the orbit, defines the Poincaré map as given by

$$P : \Re^4 \to \Re^4 \quad \mathbf{x}_{n+1} = P(\mathbf{x}_n) \tag{9}$$

where $\mathbf{x}_n$ and $\mathbf{x}_{n+1}$ are the nth and $(n+1)$th samples of $\mathbf{x}(t)$, respectively.

For a chaotic system, it is essential to know the formation of chaos due to the variation in system parameters. As a parameter

TABLE I
MACHINE PARAMETERS

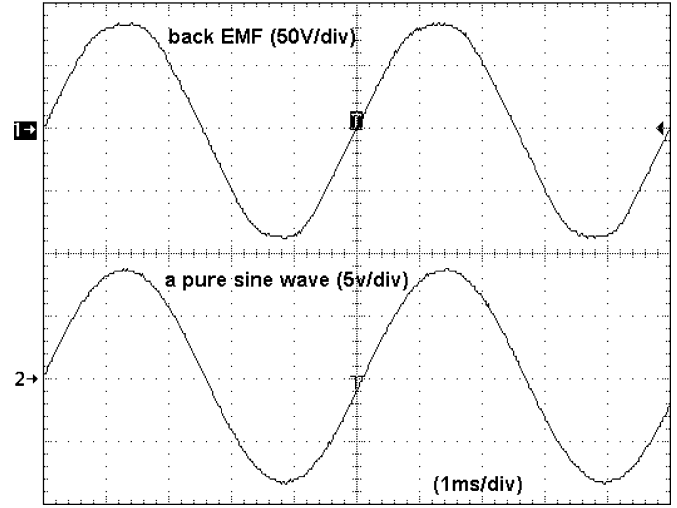| Parameter	Value
L_{ds}	25.03 mH
L_{qs}	12.26 mH
R_s	2.763 Ω
n_p	4
ψ_a	0.1432 Wb
ψ_{pm}	0.1955 Wb
δ	22°
J	1.324×10^{-3} kg·m²
B_m	4.584×10^{-3} N·m·s

Fig. 2. Measured back EMF waveform at the rated speed 1500 r/min.

is varied, a bifurcation is an abrupt change in the steady-state behavior of the system. A plot of the steady-state orbit against a bifurcation parameter is termed a bifurcation diagram. Thus, the bifurcation analysis facilitates the appraisal of the steady-state system behavior at a glance.

IV. PM SIZING AND CHAOS

It is anticipated that there are different system parameters affecting the stability and hence the formation of chaos. In this paper, the PM sizing and hence the PM flux is particularly interested.

A practical three-phase 12/8-pole DSPM machine with rotor skewing δ is used for experimentation. Its parameters are listed in Table I. Fig. 2 shows the measured back EMF waveform of the machine at the rated speed of 1500 r/min, and a pure sinusoidal waveform produced by a signal generator. Obviously, the EMF waveform is very close to be sinusoidal, indicating that the approximation for (1) is valid.

In order to experimentally verify the above derivation, the DSPM machine purposely operates at the conditions of $f = 25$ Hz, $V = 55$ V, $\alpha = 0$ and $T_m = 0$. When selecting ψ_a as the bifurcation parameter, the corresponding bifurcation diagram of the rotor speed is shown in Fig. 3. It illustrates that there exists a critical value of ψ_a for stable operation. Beyond this critical value, the DSPM machine will exhibit chaotic behaviors, namely random-like but bounded oscillations. As
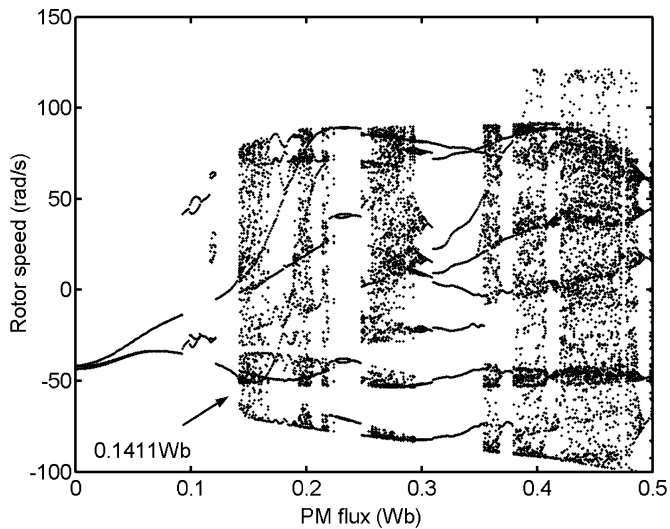
Fig. 3. Rotor speed bifurcation diagram via ψ_a.

Fig. 4. Measured chaotic waveforms and trajectories. (a) i_{ds}. (b) i_{qs}. (c) ω_r. (d) $i_{ds} - i_{qs}$ plane. (e) $i_{ds} - \omega_r$ plane. (f) $i_{qs} - \omega_r$ plane.

shown in Table I, the ψ_a of the adopted machine is 0.1432 Wb, which is beyond the critical value of 0.1411 Wb for the above operating conditions. Thus, the machine purposely operates at chaos. Fig. 4 shows the measured chaotic behaviors, including the time-domain waveforms of i_{ds}, i_{qs}, and ω_r, as well as the trajectories on the $i_{ds} - i_{qs}$, $i_{ds} - \omega_r$, and $i_{qs} - \omega_r$ planes. It can be found that the waveforms offer the typical chaotic properties, namely random-like and bounded, while the trajectories resemble a double-scroll, especially on the $i_{qs} - \omega_r$ plane. Therefore, the adopted DSPM machine exhibits chaotic behaviors at the above operating conditions, namely at reduced frequency, reduced voltage, zero phase difference, and zero driving torque, which can occur in a practical world.

Based on the above finding, the designer for DSPM machines should not only size the PMs for the sake of torque production, but also take into account the critical value of PM flux to avoid the formation of chaos.

V. CONCLUSION

This paper has analyzed the effect of PMs on the formation of chaos in DSPM machines. The key is to derive the critical value of PM flux using the Poincaré map and bifurcation diagram. Beyond this critical value, bifurcation and hence chaos are resulted. A practical three-phase 12/8-pole DSPM machine with rotor skewing has been employed for exemplification. The measured results, including both chaotic waveforms and trajectories, have verified the theoretical derivation, and confirmed the importance of this analysis.
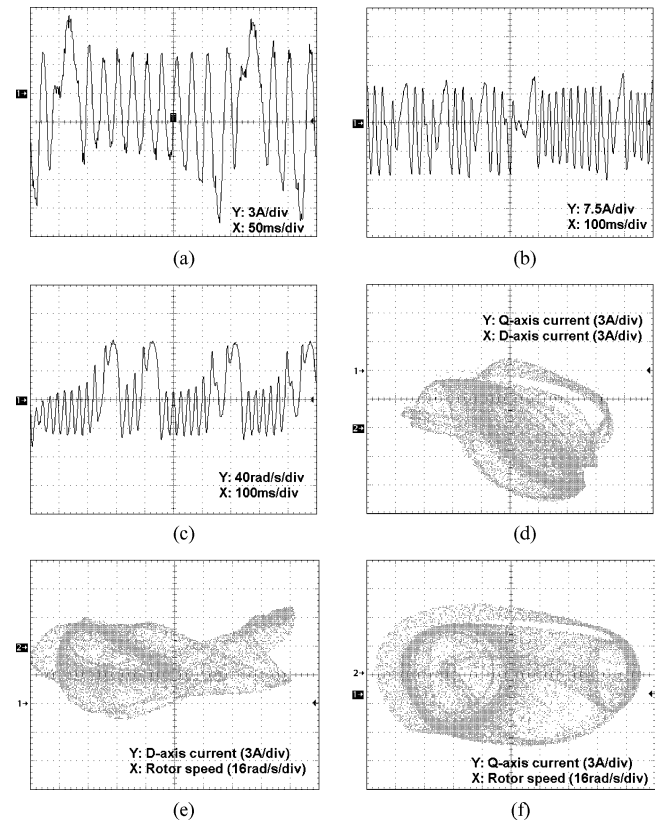
REFERENCES

[1] Y. Liao, F. Liang, and T. A. Lipo, "A novel permanent magnet motor with doubly salient structure," *IEEE Trans. Ind. Applicat.*, vol. 31, pp. 1059–1078, Sept.–Oct. 1995.
[2] M. Cheng, K. T. Chau, C. C. Chan, E. Zhou, and X. Huang, "Nonlinear varying-network magnetic circuit analysis for doubly salient permanent magnet motors," *IEEE Trans. Magn.*, vol. 36, pp. 339–348, Jan. 2000.
[3] M. Cheng, K. T. Chau, and C. C. Chan, "Design and analysis a new doubly salient permanent magnet motor," *IEEE Trans. Magn.*, vol. 37, pp. 3012–3020, July 2001.
[4] J. H. Chen, K. T. Chau, and C. C. Chan, "Analysis of chaos in current-mode controlled dc drive systems," *IEEE Trans. Ind. Electron.*, vol. 47, pp. 67–76, Feb. 2000.
[5] A. S. Bazanella and R. Reginatto, "Robustness margins for indirect field-oriented control of induction motors," *IEEE Trans. Automat. Contr.*, vol. 45, pp. 1226–1231, June 2000.
[6] N. Hemanti, "Strange attractors in brushless dc motors," *IEEE Trans. Circuits Syst. I*, vol. 41, pp. 40–45, Jan. 1994.
[7] J. H. Chen, K. T. Chau, C. C. Chan, and Q. Jiang, "Subharmonics and chaos in switched reluctance motor drives," *IEEE Trans. Energy Conversion*, vol. 17, pp. 73–78, Mar. 2002.
[8] Y. Gao and K. T. Chau, "Design of permanent magnets to avoid chaos in PM synchronous machines," *IEEE Trans. Magn.*, vol. 39, pp. 2995–2998, Sept. 2003.